



Response surface methodology: Optimization of myco-synthesized gold and silver nanoparticles by *Trichoderma saturnisporum*

Mohammed Abu-Elghait¹ · Mohamed K. Y. Soliman¹ · Mohamed Salah Azab¹ · Salem S. Salem¹ 

Received: 16 October 2023 / Revised: 20 November 2023 / Accepted: 27 November 2023
© The Author(s) 2023

Abstract

In the current study, the optimal reaction condition for fabrication of Au and Ag nanoparticles by using *Trichoderma saturnisporum* was developed. Optimization of fermentation conditions for extracellular AuNPs and AgNPs synthesis using response surface methodology was achieved. To accomplish the ideal reaction state, the green synthesis reaction's effective parameters and central composite face design were used. Precursor concentrations, pH, and temperature were found to be the most effective parameters for the fabrication of Au and Ag nanomaterials. The model's realization used a respectable foot. Normal probability plots; interaction plots, including effect plots; variance analysis (ANOVA), surface plots; contour plots; and Pareto charts were used to optimize the components. Significance threshold (5%) was used to influence all of the factors. The production process was also influenced by some of the potential connections between these factors. The recommended regression model fits the experimental data extremely well. The findings of this study looked at how much more bio-fabrication was possible with optimal fermentation conditions for the producer of AuNPs and AgNPs compared with traditional optimization techniques.

Keywords Silver nanoparticles · Gold nanoparticles · Green synthesis · Optimization

1 Introduction

Nanoparticles (NPs) have garnered a lot of attention recently for a variety of uses in biosensors, electronics, optics, catalysis, medicine, and agriculture. Due to their comparable size to biomolecules and ease of penetration, it is widely known that NPs (within the size range of a wavelength of 100 nm) are effectively used for an assortment for aims [1]. The earliest documentation of the medicinal use of gold and its compounds as medicines dates to the ancient Egypt, where it was first documented over 5000 years ago [2]. Due to its intriguing qualities including easy manufacturing and surface modification, biocompatibility, and no cytotoxicity, gold nanoparticles (AuNPs) have attracted a lot of attention [3–5]. They are very useful in the disciplines of biotechnology and biomedicine thanks to these special qualities. In truth, AuNPs offer a wide range of potential uses in nanomedicine and novel types of catalysis [6, 7]. Since it does not employ any dangerous or poisonous chemicals, the biological production of AuNPs by plant, fungi, actinomycetes,

and bacteria has gained intriguing research. However, as compared to the beginning materials, silver nanoparticles (AgNPs) exhibit markedly different characteristics, largely because of the higher surface area to volume ratio, which boosts their ability to function in biology [8–10]. Silver NPs are widely acknowledged for their specific antibacterial characteristics in addition to their strong conductivity in electricity and visual impacts [11–14]. Additionally, NPs may be produced at low pressure, temperature, and pH levels, which lessen their toxicity and expands their potential medical applications [15–17]. The production of AuNPs by fungi offers numerous advantages, including minimal use of energy, high efficiency, the absence of additional capping and stabilizing agents, ease of operation, and simplicity of separation and purification. When various fungal species or reaction circumstances are applied, it has been discovered that many fungi can produce AuNPs both within and outside of cells with varying particle compositions and characteristics [18]. Chemical and physical methods are the most often used to create NPs. However, these synthesis processes are very costly and produce toxic by-products since they use dangerous chemicals that are bad for the environment [19]. Because of its benefits over physicochemical techniques lower energy needs, non-toxic reagents, biocompatibility, simplicity of processing, better stability, elimination of unnecessary

✉ Salem S. Salem
salemsalahsalem@azhar.edu.eg

¹ Botany and Microbiology Department, Faculty of Science, Al-Azhar University, Nasr City, Cairo 11884, Egypt

processing during synthesis, and sustainability the biological method is recommended [20–22]. Physicochemical methods can result in hazardous consequences and are still somewhat costly [23–27]. Biological agents including bacteria, fungus, yeast, actinomycetes, and plants are used in the biological approach of NPs synthesis [28–31]. Numerous enzymes (metabolites) produced by biological entities decrease metallic ions through enzymatic processes [32, 33]. In general, fungi such as *V. lecanni*, *Trichoderma atroviride*, and *F. oxysporum* and actinomycetes such as *Streptomyces* and other bacteria *Rhodococcus* spp. and *Thermomonospora* were also used to synthesize AuNPs intra- and extracellularly [34]. However, the formation of AuNPs is still scarce [35].

Assessment of the interactions between reaction variables that affect the creation of AgNPs and how they can be optimized is required for the effective reduction of metal ions as silver (Ag^+) to AgNPs (Ag^0) when using various bioreducers. Optimization constitutes one of the crucial steps in the development of a formation protocol [36].

Recent investigation has shown that altering the biosynthetic reaction's processing variables, such as mixing ratio, temperature, aeration, pH, and incubation time, may improve the production of NPs that have various morphologies [37, 38]. The procedure of fermentation by microorganisms has typically been improved by evaluating the effect of one-variable at a time (OVAT) on a controlled action. In this strategy, one parameter is altered while maintaining the levels of the other variables [39–41]. The Plackett–Burman design offers a quick and efficient method for determining what factors need that must be employed in optimization [42, 43].

As a result, it was unable to identify the interactions between the various factors and the full impact of each parameter on the answer. Additionally, using this kind of study necessitates doing several experiments, which adds to the needed time and money. Technique for responding to surfaces, a well-known statistical analysis technique, statistical analysis (RSM), is used to optimize the components of the medium along with various significant variables involved in the generation of microbial compounds [44–46]. Consequently, RSM might produce higher-quality findings while reducing expenses and time [47]. Furthermore, RSM describes the estimation of ideal circumstances by analysing the relationship between all of the variables in a process [48]. In order to maximise the creation of NPs, a face centred central composite design (FCCCD) was performed [49].

2 Material and methods

2.1 Microorganism

From agricultural soil, the fungus *Trichoderma saturnisporum* was isolated. Malt extract agar (MEA) had been employed to isolate the fungus strain and was grown at 28 °C for 5 days.

The discovered isolate was genetically identified via molecular identification utilizing genomic DNA and its region of amplification. The discovered fungal isolates' ITS sequences have been contrasted to the ones in the GenBank databases.

2.2 Biosynthesis of AgNPs and AuNPs

Following that, both AgNPs and AuNPs were created using the cell-free filtrate. Preparing for mixing, 1 mmol each of AgNO_3 and HAuCl_4 was purchased from Sigma-Aldrich, USA. Other chemicals, culture media and reagents used in this study were purchased from Modern Lab Co. Alongside *Trichoderma saturnisporum*'s cell-free filtrate as well as incubation for 72 h at 28 °C upon a vibrating shaker (120 rpm) in dark conditions, the pH was raised to 10 to AgNPs while 5 for AuNPs, accordingly, AgNPs along with AuNPs both displayed brown and violet hues after the incubation period. The finished product underwent separation and was oven-dried for 24 h at 200 °C. Then, the AgNPs and AuNPs by-products were collected, and the focus was on further analysis.

2.3 UV–Vis investigation

In order to assess the influence of multiple variables upon the biosynthesis of AgNPs along with AuNPs, their exterior plasmon resonance peak frequencies were measured through the use of an absorbance, the spectral scan with a double-beam UV–Vis spectra on the JASCO, V-630, UV–Vis Spectrophotometer (JASCO-INTERNATIONAL-CO, LTD) at a spatial resolution of 1 nm within the length of the wave range of 200 and 800 nm. Due to the variety of factors such as the size and concentration of the nanoparticles utilized in the experiment, the UV–Vis spectrum may fluctuate. In order to ascertain whether the creation of nanoparticles was rising or falling, the absorbance intensity was employed.

2.4 Optimization studies for nanoparticle production

The variables relating cell-free filtrate and the initial components of nanoparticles (silver nitrate as well as chloroauric acid) were optimized during optimization experiments. Subsequently employing a single factor at a time (OFAT) technique, the impacts of various incubation times, precursor concentrations, pH values, incubation temperatures, shaking for efficiency, and influence of biomass weight had been screened. Every single factor underwent modification whereas other factors remained untouched. Response to change surface statistical procedure was subsequently employed for assessing the relevance of all of these factors and how they correlated with the other factors and determine

the most significant factors to design the experiment at Plackett–Burman design (PBD).

2.5 Effect of different incubation periods

The biomass filtrate of the fungal isolate was mixed with 1 mmol AgNO_3 or HAuCl_4 for different incubation periods as 24, 48, 72 and 96 h. Myco-synthesized nanoparticles were characterized at the end of each incubation time by UV–visible spectroscopy.

2.6 Precursor concentration

The concentration of the precursor affects the quantity of the nanoparticles produced. Various concentrations of AgNO_3 and HAuCl_4 were tested (0.5, 1, 2.0 and 3.0 mmol) to select the best substrate concentration. Biosynthesized nanoparticles were analysed at maximum surface plasmon resonance peak by UV–visible spectroscopy.

2.7 Effect of different pH values

The generation of the enzymes needed for the creation of nanoparticles is greatly influenced by pH. Different pH ranging from 5 to 9 for AuNPs and from 6 to 10 for AgNPs were used to study the influence of pH on nanoparticle production from the fungal isolate in the presence of 1 mmol AgNO_3 or HAuCl_4 as substrate precursors; biosynthesized nanoparticles were analysed at maximum surface plasmon resonance peak by UV–visible spectroscopy.

2.8 Effect of different incubation temperatures

Temperature plays a very important role in all biological reactions. Temperatures ranging between 25, 35 and 45 °C were used in optimisation tests with respect to temperature of cell-free filtrate with 1 mmol AgNO_3 or HAuCl_4 for production of silver and gold nanoparticles. A specified wavelength of UV–visible spectroscopy for absorption was used to analyse the substance being investigated.

2.9 Effect of shaking for productivity

The effect of shaking and static condition between precursors and cell-free filtrate (CFF) was examined by preparing CFF then incubated at 120 rpm and at static condition. The myco-synthesized nanoparticles were characterized at the end of incubation periods to determine the best condition for production.

2.10 Effect of biomass weight

Different produced biomass of the most potent isolates was added to the same volume of distilled water and same condition. Weight was 10, 20 and 30 g/100 ml distilled water, and the resulted nanoparticles were analysed at maximum surface plasmon resonance peak by UV–visible spectroscopy.

2.11 Designing experiments and optimising them using RSM

Utilising Design Expert software (Version 10.0.3.1, Stat-ease, Minneapolis, USA), response surface approach was used to examine an estimated functionality relationship across the three most important factors. With the use of CCD, all the variables involved were further minimised [50].

2.12 Statistical optimization by CCD model

RSM was used to do the statistical optimization. The CCD, which illustrates the connection among the parameters and response (precursors concentrations, pH, temperature and nanoparticles (silver and gold) synthesis), is a particularly popular and extremely successful RSM approach employed in optimization. Cube points were utilised to fit a linearity (first order) approach, axial points to calculate the quadratic (second-order) polynomial terms and centre cube points to determine the quadratic effects between high and low levels of each variable, as well as for assessing the pure experimental error.

The model may provide optimization curves that foretell the ultimate best configurations of the interacting parameters that boost nanoparticle production according to the CCD statistical data analysis's results in math and graphics. The effects of precursor conc., temp. and pH were calculated using a two-level, five-factor (2^5) complete factorial CCD. The CCD matrix, which includes the actual results of the experiment's runs at each factor's five levels, is presented in Tables 1 and 2. The significance level of the straight line, quadratic and relationship factors was assessed using analysis of variability (ANOVA).

2.13 Experimental design and setup

An Erlenmeyer flask with a working volume of 200 mL and a volume of 250 mL was used for each experiment. To identify the influence of precursors conc., pH and temperature on the creation of nanoparticles by *Trichoderma saturnisporum*, 14 runs of Erlenmeyer flasks were divided into 20 for silver and 20 for gold. Concentration at 0.2, 0.6, 1.0, 1.4 and 1.8 mM of AgNO_3 and HAuCl_4 precursors were added to the same volume

Table 1 Design and outcomes of an experimental study that sought to optimise 2^5 complete factorial CCDs of pH, temperature and precursor concentration in response to both high and low levels of interacting variables for AgNPs

| RunOrder | PtType | Blocks | PH | TEMP | CONC | Absorbance at 430 nm |
|----------|--------|--------|----|------|------|----------------------|
| 1 | 0 | 1 | 8 | 35 | 1 | 0.841 |
| 2 | 1 | 1 | 7 | 40 | 1.4 | 0.752 |
| 3 | 1 | 1 | 9 | 40 | 1.4 | 0.745 |
| 4 | 1 | 1 | 9 | 40 | 0.6 | 0.565 |
| 5 | 1 | 1 | 7 | 40 | 0.6 | 0.456 |
| 6 | 1 | 1 | 7 | 30 | 0.6 | 0.211 |
| 7 | -1 | 1 | 10 | 35 | 1 | 0.786 |
| 8 | 0 | 1 | 8 | 35 | 1 | 0.799 |
| 9 | 1 | 1 | 9 | 30 | 0.6 | 0.635 |
| 10 | 1 | 1 | 7 | 30 | 1.4 | 0.421 |
| 11 | 0 | 1 | 8 | 35 | 1 | 0.821 |
| 12 | -1 | 1 | 8 | 35 | 1.8 | 0.765 |
| 13 | 1 | 1 | 9 | 30 | 1.4 | 0.698 |
| 14 | -1 | 1 | 6 | 35 | 1 | 0.568 |
| 15 | -1 | 1 | 8 | 45 | 1 | 0.514 |
| 16 | -1 | 1 | 8 | 35 | 0.2 | 0.233 |
| 17 | 0 | 1 | 8 | 35 | 1 | 0.824 |
| 18 | 0 | 1 | 8 | 35 | 1 | 0.831 |
| 19 | 0 | 1 | 8 | 35 | 1 | 0.833 |
| 20 | -1 | 1 | 8 | 25 | 1 | 0.714 |

Table 2 Design and outcomes of an experimental study that sought to optimise 2^5 complete factorial CCDs of pH, temperature and precursor concentration in response to both high and low levels of interacting variables for AuNPs

| RunOrder | PtType | Blocks | PH | TEMP | CONC | Absorbance at 550 nm |
|----------|--------|--------|----|------|------|----------------------|
| 1 | 0 | 1 | 4 | 35 | 1 | 0.088 |
| 2 | 1 | 1 | 6 | 35 | 0.2 | 0.063 |
| 3 | 1 | 1 | 6 | 25 | 1 | 0.765 |
| 4 | 1 | 1 | 7 | 30 | 1.4 | 1.123 |
| 5 | 1 | 1 | 5 | 40 | 0.6 | 0.156 |
| 6 | 1 | 1 | 5 | 30 | 0.6 | 0.566 |
| 7 | -1 | 1 | 6 | 35 | 1 | 0.965 |
| 8 | 0 | 1 | 6 | 35 | 1 | 1.012 |
| 9 | 1 | 1 | 6 | 35 | 1 | 0.988 |
| 10 | 1 | 1 | 5 | 40 | 1.4 | 0.126 |
| 11 | 0 | 1 | 7 | 30 | 0.6 | 0.496 |
| 12 | -1 | 1 | 6 | 45 | 1 | 0.223 |
| 13 | 1 | 1 | 8 | 35 | 1 | 0.622 |
| 14 | -1 | 1 | 6 | 35 | 1 | 0.978 |
| 15 | -1 | 1 | 6 | 35 | 1.8 | 0.209 |
| 16 | -1 | 1 | 5 | 30 | 1.4 | 0.082 |
| 17 | 0 | 1 | 6 | 35 | 1 | 0.968 |
| 18 | 0 | 1 | 7 | 40 | 1.4 | 0.865 |
| 19 | 0 | 1 | 7 | 40 | 0.6 | 0.455 |
| 20 | -1 | 1 | 6 | 35 | 1 | 0.986 |

of cell-free filtrate. pH at 6, 7, 8, 9 and 10 for AgNPs and at 4, 5, 6, 7, and 8 for AuNPs. Finally, different condition of temperature was used for AgNPs and AuNPs at 25, 30, 35, 40 and 45 °C.

2.14 Response surface methodology validation

The Minitab® DoE statistical package's response optimizer, a tool, was utilized for developing the optimization curves in order to identify the precise combinations of the interacting parameters that would enhance NPs' productivity. On a scale of 0 to 1, the anticipated settings were evaluated for their capacity to optimize the response using individual (*d*) and composite (*D*) desire. Additional confirmation experiments were conducted after this step to verify the projected parameters produced by the curves of optimization.

2.15 Statistical analysis

Applying Minitab® version-18 (2017) reinforced with software for statistics and graphics, every experimental outcome for RSM models were created and evaluated. After that, the model's strength was evaluated by looking at the ANOVA determination coefficient (R^2). The ANOVA test was utilised to assess the data given as a mean and standard deviation. At the 0.05 probability level, Fisher test was utilised to compare the means across the groups. Following that, the surface plots were plotted using Sigma Plot v14.0 SPW.

3 Results and discussion

In the development of a biotechnology production process of technologically significant compounds, incubation temperature, agitation, aeration, pH, oxygen levels and medium composition have to be tuned to enhance growth and yield [51, 52].

3.1 Effect of different incubation periods, precursor concentration, different incubation temperature, shaking and biomass weight using OFAT method

As shown in Fig. 1A, the optimal incubation time to produce maximum extracellular AgNPs and AuNPs was when the biomass filtrate of *Trichoderma saturnisporum* treated with 1.0 mM AgNO₃ and HAuCl₄ solution was 72 h, which gave the highest optical density reading. The effect of different precursor concentration of AgNO₃ and HAuCl₄ (Fig. 1B) showed that the optimum substrate concentration for *Trichoderma saturnisporum* was 1.0 mM for maximum productivity of AgNPs and AuNPs which was characterized by UV–visible spectra.

Effect of different pH values on biosynthesis of AgNPs and AuNPs Biosynthesis of AgNPs and AuNPs was influenced by pH of the mixture between biomass filtrate and silver nitrate

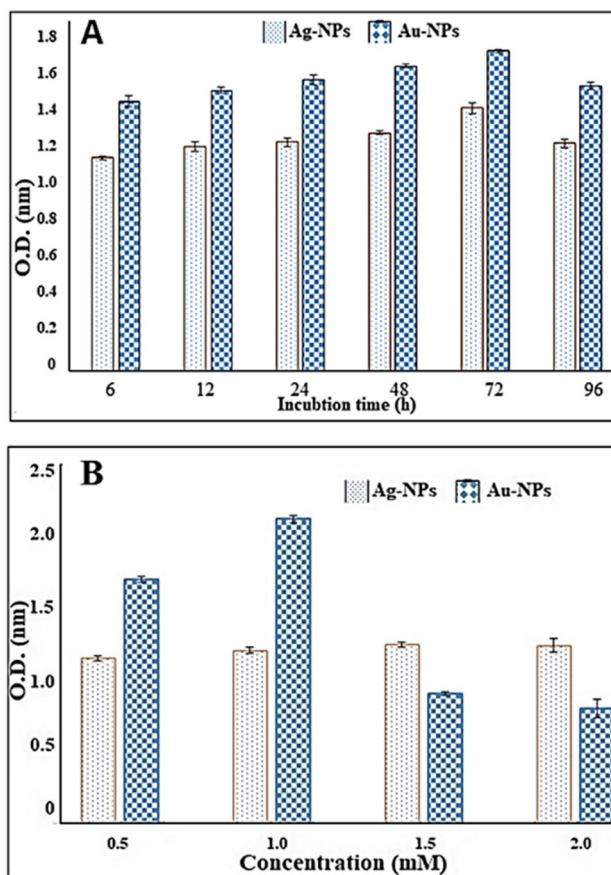


Fig. 1 Effect of incubation time (A) and different conc. of AgNO₃ and HAuCl₄ (B) on biosynthesis of AgNPs and AuNPs by *T. saturnisporum*

and chloroauric acid. Data represented graphically in Fig. 2A revealed that the absorbance increased by increasing pH value till pH 9 which is the maximum peak for synthesising AgNPs. It is evident that *T. saturnisporum* produced metabolites that are more stable in alkaline solutions than in acidic ones when used to cap AgNPs. However, the optimum pH value for bio fabricated AuNPs was 8 for *Trichoderma saturnisporum*.

Effect of different temperatures on biosynthesis of AgNPs and AuNPs Temperature is an essential environmental factor affecting nanoparticle production, so the effect of different temperatures on the production of AgNPs and AuNPs formed by *T. saturnisporum* was studied. The maximum productivity of AgNPs and AuNPs was attended at 35 °C when compared with other temperatures (Fig. 2B).

Effect of shaking for productivity of AgNPs and AuNPs Data in Fig. 3A revealed that the productivity of AgNPs and AuNPs characterized by UV–visible spectra was not significantly affected by different agitation on shaker at 120 rpm or static condition by *Trichoderma saturnisporum*.

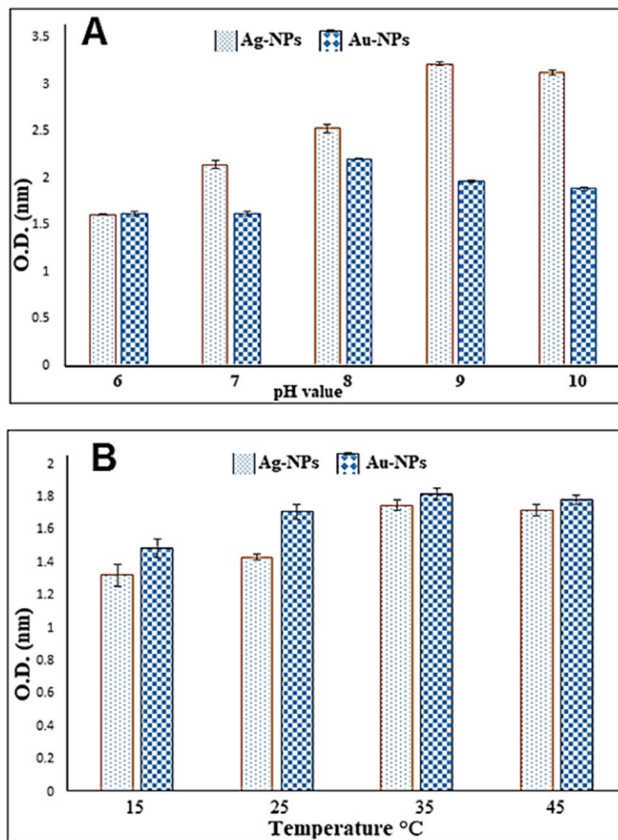


Fig. 2 Effect of different pH (A) and temperatures (B) on biosynthesis of AgNPs and AuNPs by *T. saturnisporum*

Effect of different biomass weight of fungal mycelium on production of AgNPs and AuNPs The biomass weight of fungal mycelium of *Trichoderma saturnisporum* had no critical effect on biosynthesis of AgNPs and AuNPs represented in Fig. 3B.

Three significant factors (pH, temperature, and precursor concentration) were measured after 72 h and designed by central composite design on Minitab program to study which together can obtain the best optimum conditions not only to tremendously help in the development of *Trichoderma saturnisporum* but also to raise the productivity and output of silver and gold nanoparticles.

3.2 Optimization of *Trichoderma saturnisporum* filtrate formation for AgNPs and AuNPs biosynthesis by RSMS

The Plackett–Burman design (PBD) is used to screen the important factors in the creation of AgNPs and AuNPs. Table 2 displays the effects of 20 runs with a variety of the independent factors on the creation of AgNPs and AuNPs. Tables 3 and 4 demonstrate the results of statistical ANOVA on the data acquired for the creation of AgNPs and AuNPs.

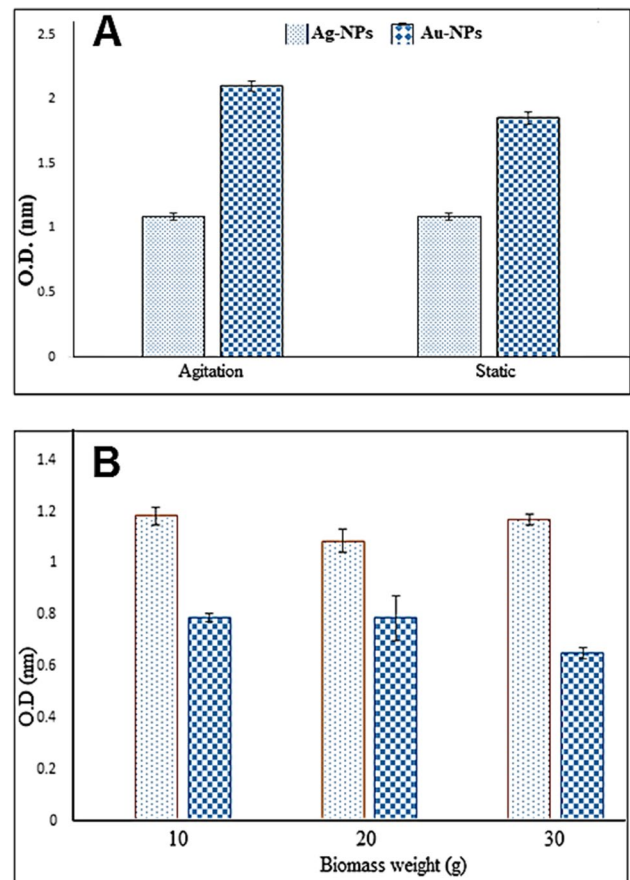


Fig. 3 Effect of different shaking (A) different biomass weight (B) on biosynthesis of AgNPs and AuNPs by *T. saturnisporum*

Table 3 Analysis of variance of three factors (pH, temperature and concentration) of AgNPs produced by *Trichoderma saturnisporum*. F value = 6.24; $R^2 = 84.88$: values of “prob > F ” less than <0.05 denotes the model are significant

| Source | DF | Adj-SS | Adj-MS | F value | P value |
|---------------------|----|----------|----------|-----------|-----------|
| Model | 9 | 0.620785 | 0.068976 | 6.24 | 0.004 |
| Linear | 3 | 0.302844 | 0.100948 | 9.13 | 0.003 |
| PH | 1 | 0.095945 | 0.095945 | 8.68 | 0.015 |
| TEMP | 1 | 0.001463 | 0.001463 | 0.13 | 0.724 |
| CONC | 1 | 0.205436 | 0.205436 | 18.58 | 0.002 |
| Square | 3 | 0.259294 | 0.086431 | 7.82 | 0.006 |
| PH*PH | 1 | 0.051922 | 0.051922 | 4.70 | 0.055 |
| TEMP*TEMP | 1 | 0.094150 | 0.094150 | 8.52 | 0.015 |
| CONC*CONC | 1 | 0.203400 | 0.203400 | 18.40 | 0.002 |
| Two-way interaction | 3 | 0.058647 | 0.019549 | 1.77 | 0.217 |
| PH*TEMP | 1 | 0.044850 | 0.044850 | 4.06 | 0.072 |
| PH*CONC | 1 | 0.008646 | 0.008646 | 0.78 | 0.397 |
| TEMP*CONC | 1 | 0.005151 | 0.005151 | 0.47 | 0.510 |
| Error | 10 | 0.110564 | 0.011056 | - | - |
| Lack-of-fit | 5 | 0.109515 | 0.021903 | 104.42 | 0.000 |
| Pure error | 5 | 0.001049 | 0.000210 | - | - |
| Total | 19 | 0.731349 | - | - | - |

Table 4 Analysis variance of three factors (pH, temperature, and concentration) of AuNPs produced by *Trichoderma saturnisporum*. *F* value=23.41; *R*²=95.47: values of prob>*F* less than <0.05 denotes that the model are significant

| Source | DF | Adj-SS | Adj-MS | <i>F</i> value | <i>P</i> value |
|---------------------|----|---------|---------|----------------|----------------|
| Model | 9 | 2.68977 | 0.29886 | 23.41 | 0.000 |
| Linear | 3 | 0.82445 | 0.27482 | 21.52 | 0.000 |
| PH | 1 | 0.59175 | 0.59175 | 46.35 | 0.000 |
| TEMP | 1 | 0.19119 | 0.19119 | 14.97 | 0.003 |
| CONC | 1 | 0.04151 | 0.04151 | 3.25 | 0.102 |
| Square | 3 | 1.55704 | 0.51901 | 40.65 | 0.000 |
| PH*PH | 1 | 0.62541 | 0.62541 | 48.98 | 0.000 |
| TEMP*TEMP | 1 | 0.38018 | 0.38018 | 29.78 | 0.000 |
| CONC*CONC | 1 | 1.13499 | 1.13499 | 88.89 | 0.000 |
| Two-way interaction | 3 | 0.30828 | 0.10276 | 8.05 | 0.005 |
| PH*TEMP | 1 | 0.00056 | 0.00056 | 0.04 | 0.838 |
| PH*CONC | 1 | 0.30070 | 0.30070 | 23.55 | 0.001 |
| TEMP*CONC | 1 | 0.00702 | 0.00702 | 0.55 | 0.475 |
| Error | 10 | 0.12768 | 0.01277 | - | - |
| Lack-of-fit | 5 | 0.12623 | 0.02525 | 87.13 | 0.000 |
| Pure error | 5 | 0.00145 | 0.00029 | - | - |
| Total | 19 | 2.81745 | - | - | - |

These results pointed out that the model’s *F*-values for AgNPs and AuNPs, respectively, were 6.24 and 23.41, and its *p*-values were 0.004 and 0.000. In addition, the significant model terms (*p*-value < 0.05) for AgNPs were linear CONC and square CONC*CONC. The model’s determination coefficient (*R*²) was 84.88, demonstrating a very strong fit between the actual and predicted amounts of AgNP biosynthesis and suggesting that the model is trustworthy for this mechanism. Each independent variable’s significance was determined by calculating its probability value; as a result, a factor’s importance is indicated by a *p*-value that is less than 0.05. The range from 0 to 1 has always been *R*². The model is more potent, and the expected result is great if the coefficient *R*² is near to 1 [53]. On the other hand, the significant terms for AuNPs were linear PH as well as TEMP and square PH*PH, TEMP*TEMP and CONC*CONC. Additionally, significant value with two-way interaction PH*CONC. However, the *R*² of the equation was 95.47, demonstrating a very strong fit between the measured and projected values of AuNP biosynthesis and suggesting that the model is trustworthy for this process. An indicator of how much variation there was in the measured response rates was the *R*² value, which is always from 0 to 100. The strength of the model and the accuracy of its response prediction increase as *R*² approaches 100 [54]. The measured and anticipated outcomes

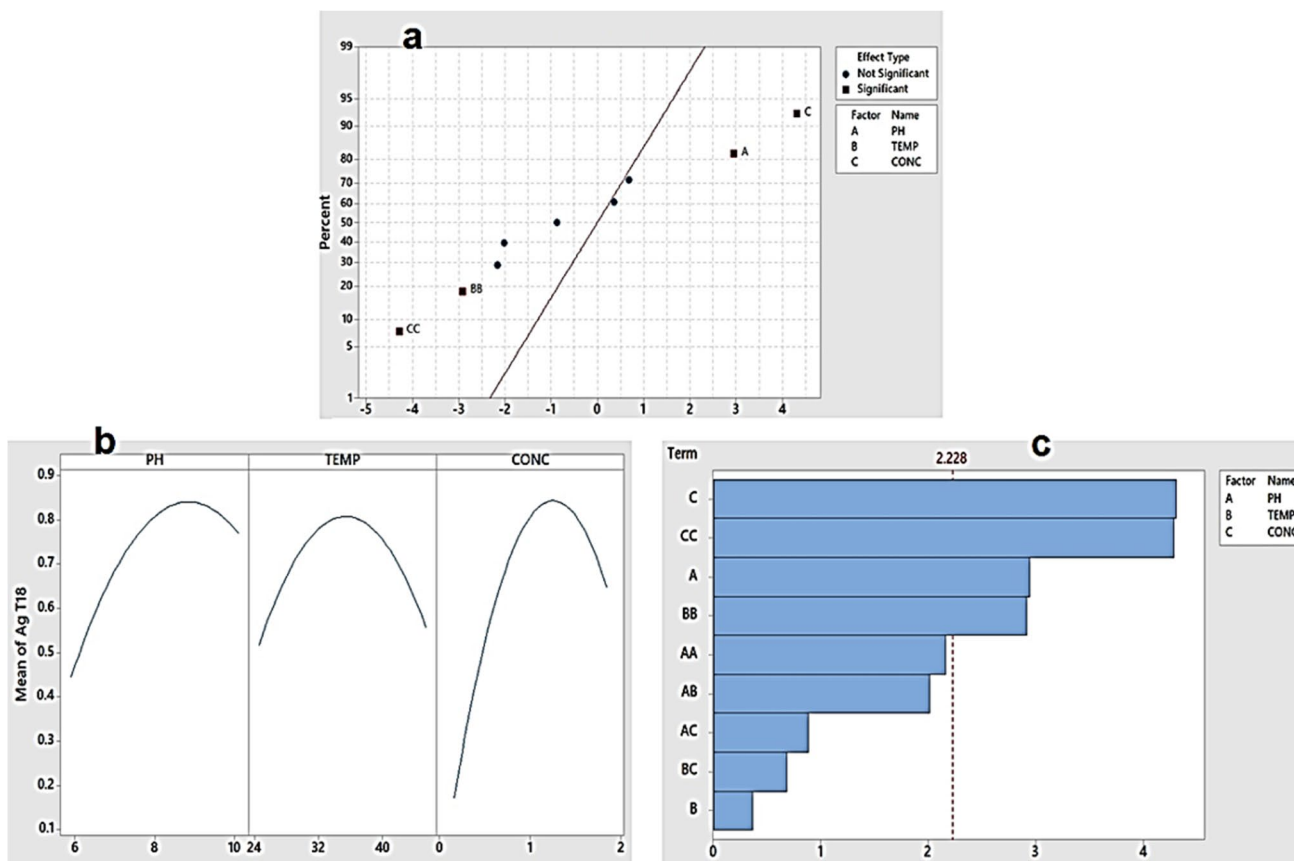
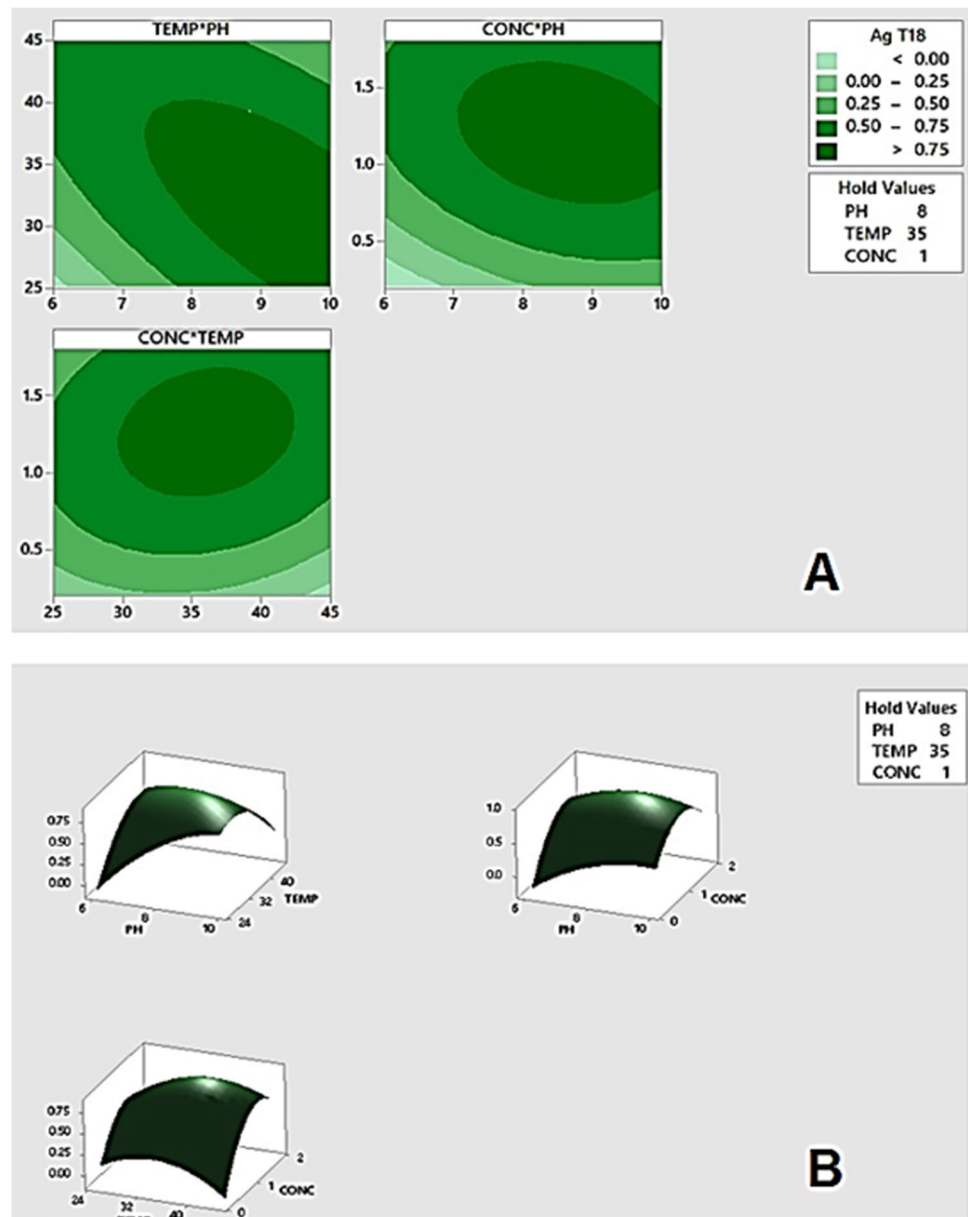


Fig. 4 Normal plot (a), mean plot (b) and Pareto chart (c) of standardized effects of AgNPs produced by *T. saturnisporum*

Fig. 5 Contour plot (A) and surface plot (B) of AgNPs produced by *T. saturnisporum*



of the creation of AgNPs and AuNPs were well in agreement, as shown by the model R^2 values of 84.44 and 95.47%. When calculating the signal to ratio of noise, the model's appropriate precision was 31.28; however, it is ideal to have more than 4 [55]. A relatively low rate of variance coefficient of 6.95% suggested that the model trials were more accurate and reliable. As a result, this model might be utilised to somewhat accurately explore the design space.

3.3 Response surface methodology for AgNPs by *T. saturnisporum*

The genuine (actual) influence of each term is determined by the normal probability plot, which also indicates whether or

not the findings were an outcome of chance (randomness). A significant departure from normalcy could be found and shown using the residuals normal probability plot [56]. In addition, normal probability plots identify whether the term has a positive or negative influence on the answer; a positive effect denotes that a rise in the factor produces an increase in the response, while a negative effect denotes the opposite. Each effect is denoted by just one point on the plot; points near a fitted line (which denotes the position where the effects were zero) indicate estimated variables that have no discernible impact on the outcome, whereas points far from the line that was fitting represent the true (real) term impact. Concentration (C), pH (A) and temp (B) are the three key terms. Their contribution's placement on the right side of the image (Fig. 4a) further indicates that it

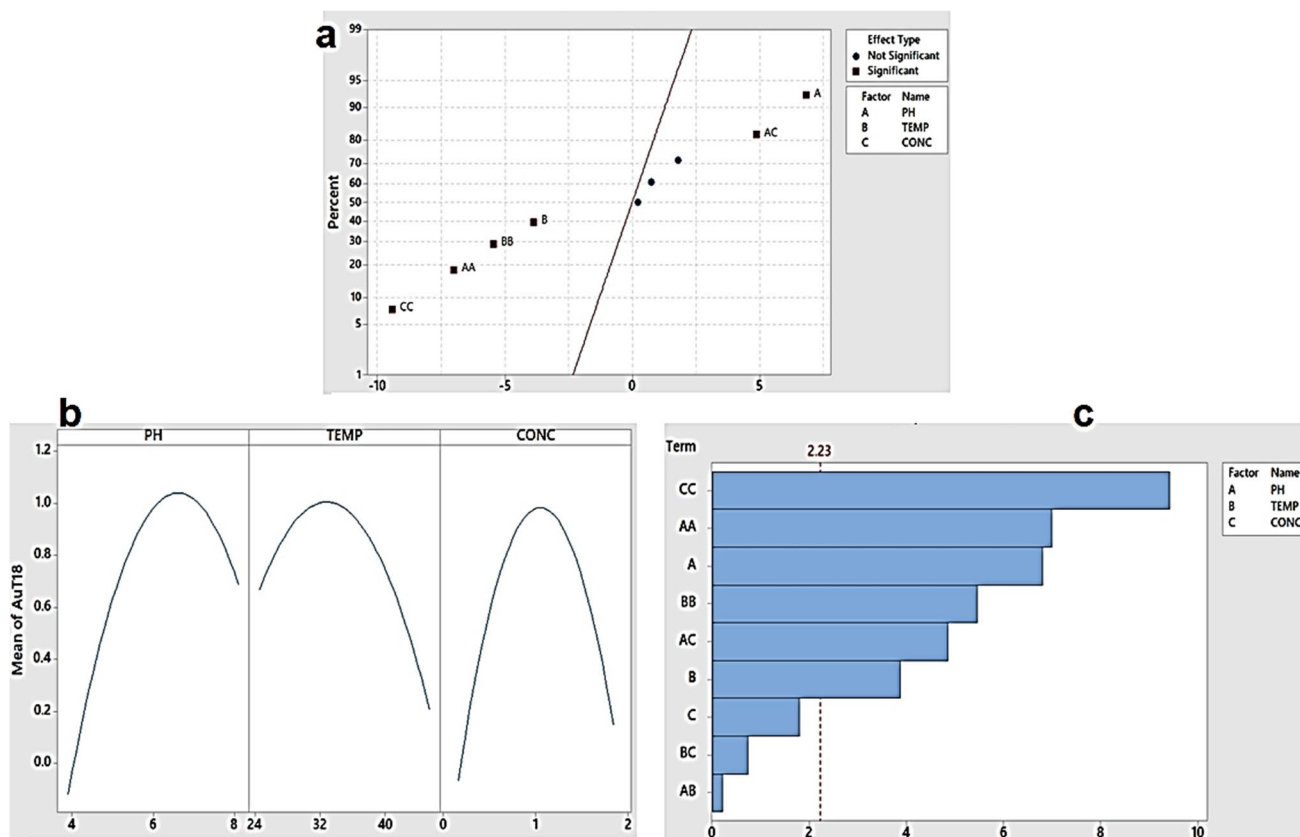


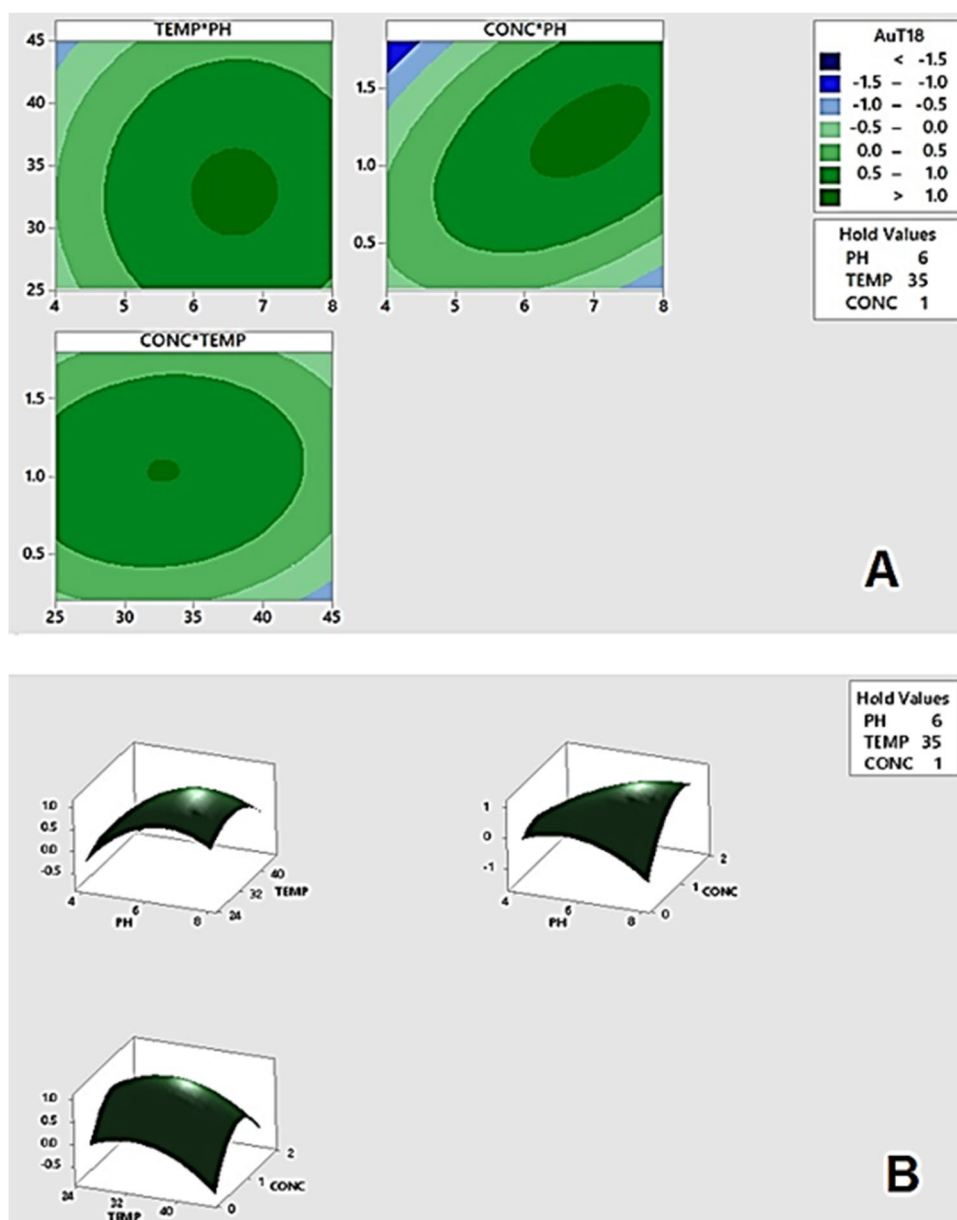
Fig. 6 Normal plot (a), mean plot (b) and Pareto chart (c) of standardized effects of AuNPs produced by *T. saturnisporum*

had a favourable impact. However, the relationships between temp (BB) and concentration (CC) are both placed to the left of the fit line, demonstrating a markedly adverse impact on the synthesis of AgNPs. Parallel to what has been observed in other investigations, AgNO₃, and pH the shielding agent, affected the size of the nanoparticles produced [57, 58]. The average variances between high and low values within every factor are displayed on the major effect plots (Fig. 4b), which were created to reflect the findings of the prediction assessment. The findings showed that there was a substantial difference between the high and low ranges of pH, concentration and temperature values. The differences in NP synthesis between both high and low amounts of each component are explained by main effects graphs [59]. The relative significance and importance of the major and effects of interaction were assessed using the Pareto chart (Fig. 4c). After 72 h, the Pareto chart plot was used to assess the factors that affect how AgNPs biosynthesize. The main impacts of concentration (C), pH (A) and temperature (B), as well as their interactions (AA, BB, CC, AB, AC, and BC), have been extended beyond the line of reference in the Pareto graph of the standardised effects for AgNP synthesis, demonstrating the significant impact of these variables at a level equal to $p \leq 0.05$. The column length of every parameter indicates the significance level of each term.

3.4 Contour plots of AgNP synthesis

The form that displays the matching contour plot reflects whether or not a relationship amongst each of the independent variables is significant. Every response surface plot reflects the effects from the two independent factors while keeping the remaining variables at zero [42]. Contour plots were made (Fig. 5A) based on the significance of the main and two-way interaction impacts in order to graphically depict the growing AgNP synthesis of each two-factor while maintaining the third component, which is not shown in the plot, stable. The contour chart is a graph with two dimensions where all points from each depicted element that has the same response value are joined to produce contour lines that range from the smallest to the largest response (count) levels. Surface plots for AgNP synthesis (Fig. 5B). A surface-wireframe diagram is a three-dimensional chart that shows how the response and the two interdependence process elements are related to one another. The optimal peaks of the best value responses are displayed on a 3D grid (wire-frame) representation of the relationship. Understanding the primary and interaction factor impacts may be accomplished using functional response area plots [60]. The numbers preceding that line

Fig. 7 Contour plot (A) and surface plot (B) of AuNPs produced by *T. saturnisporum*



have no significant impact, and the Pareto charts and normal probability plots reflected the least statistically significant effect [61].

3.5 Response surface methodology for AuNPs by *T. saturnisporum*

The primary terms for pH (A) and temperature (B) and their interaction (AA, BB, CC and AC) are distant from the fitted straight line, suggesting a highly substantial influence. Additionally, the impact of these variables was positive since it is situated on the right portion of the diagram (Fig. 6a). Additionally, the interactions between pH (AA), temperatures (BB)

and concentration (CC) are all to the left of the suited line, demonstrating a considerable detrimental impact on AuNPs biofabrication. The average variances between low and high values within each component are shown in the major effect plots (Fig. 6b), which were designed to illustrate the outcomes of the prediction analysis. It was discovered that there were considerable differences between low and high levels in pH values, temperature and concentration. The main effects of pH (A), temperature (B) and concentration (C) and their interactions (AA, BB, CC, AC, AB and BC) were all significant at the level of $p < 0.05$, with the exception of concentration (C) and the interaction of AB, BC, while the length of the column indicates the order of significance of each term (Fig. 6c).

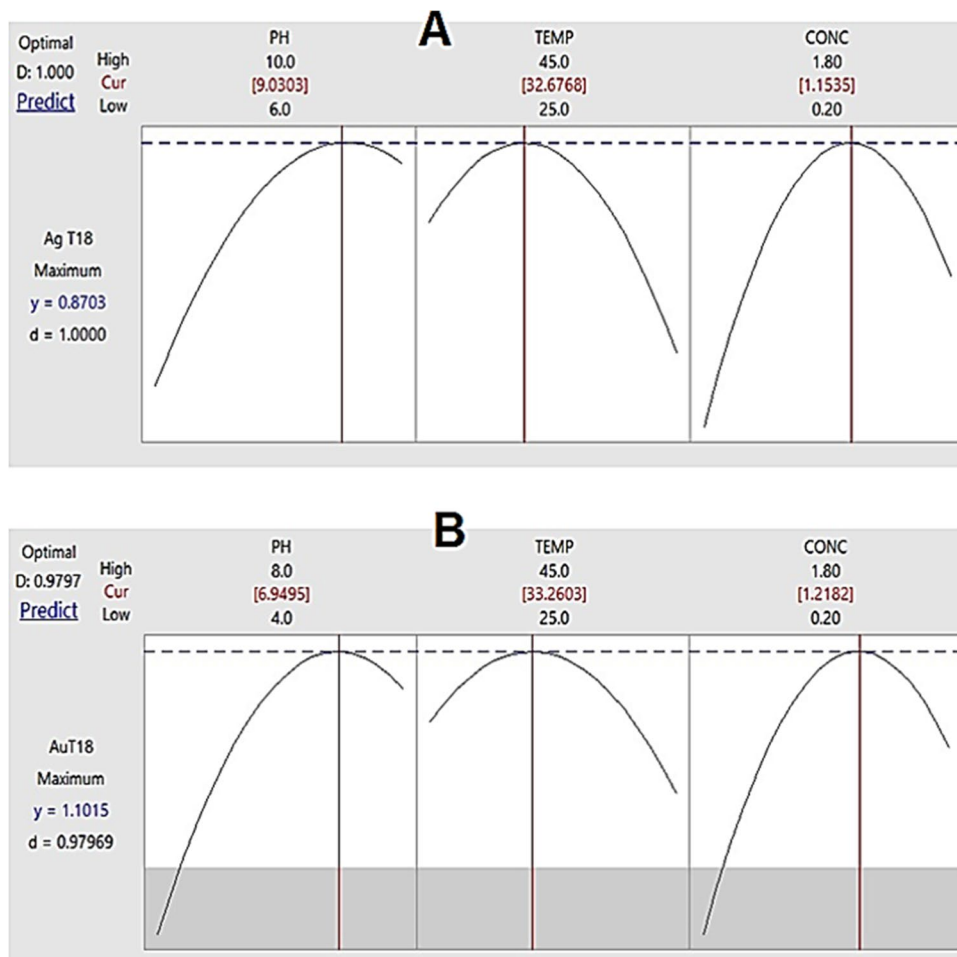
3.6 Contour plots of AuNPs synthesise

Contour and surface plots of AuNPs synthesise (Fig. 7A and B) show the surface plots and contour of AuNP synthesis between comparable encounters that follow the same pattern, where the biosynthesis of AuNPs increased to high level at pH 7 at 30 °C and 1.4 mmol of H₂AuCl₄. Nevertheless, increasing or decreasing of these parameters would decline the productivity of gold NP. According to Shakouri et al. (2016), the largest amount of gold nanoparticles was produced 96 h after 2.50 mM Au ions were incubated with *A. flavus* filtrate at 28 °C [62]. The number of AuNPs formed responded by increasing the absorbance at 550 nm. With a large level of salt concentration of 5 mM and 48 h of incubation at 30 °C, Au ion reduction increased [63]. In another study, the researchers utilized PBD to maximize the formation of the biosurfactant made by *B. subtilis*, which was used for producing AuNPs and AgNPs. Inoculum size and pH for AgNPs and AuNPs biosynthesis and ammonium

ferric citrate were the only four of the 11 variables that were demonstrated to substantially influence culture development [64]. Concentration of AgNO₃ (mM), shaking rate (rpm), incubation temperature (°C) and pH identified the effective parameters for biosynthetic optimization of AgNP generated by *Penicillium citrinum* utilizing BBD. They discovered that the resultant model's R² value was 0.8894, showing a strong connection between the predicted and observed data. They came to the conclusion that *Penicillium citrinum* might produce AgNPs under ideal circumstances at a reasonable cost-effectively and quickly [65].

The response optimizer programme was used to create the optimisation curves (Fig. 8 A and B) that show the final optimal values for the parameters that maximise the synthesis of AgNPs and AuNPs. AgNPs pH 9.0, temperature 32.6 °C and concentration 1.15 mmol were the ideal conditions for the preparation and incubation of triple repeated confirmatory runs. While the pH, temperature and concentration of AuNPs are 6.94, 33.2 °C and 1.21 mmol.

Fig. 8 Optimal predict of AgNPs (A) and AuNPs (B) produced by *T. saturnisporum*



4 Conclusions

The current work expanded the use of *T. saturnisporum* supernatant for the biosynthesis of AgNPs and AuNPs. The “one factor-at-a-time” optimization technique was used to optimize the biomanufacturing procedure. The settings were optimized using the response surface methods to produce highly synthesized AgNPs and AuNPs. The outcomes showed that the reaction parameter adjustment was indeed required and had a direct impact on the fabrication process. Predicted values have been verified and the model’s fitness was confirmed. Lastly, pH 9.0, 32.6 °C and 1.15 mmol of concentration were the ideal conditions for AgNPs biosynthesis. While the pH, temperature and concentration of AuNPs are 6.94, 33.2 °C and 1.21 mmol.

Author contribution Conceptualization: Mohammed Abu-Elghait, Mohamed K.Y. Soliman, Mohamed Salah Azab and Salem S. Salem; methodology and resources: Mohammed Abu-Elghait, Mohamed K.Y. Soliman and Salem S. Salem; validation and visualization: Mohammed Abu-Elghait, Mohamed K.Y. Soliman, Mohamed Salah Azab and Salem S. Salem; formal analysis: Mohammed Abu-Elghait, Mohamed K.Y. Soliman, Mohamed Salah Azab and Salem S. Salem; writing—original draft preparation: Mohammed Abu-Elghait, Mohamed K.Y. Soliman and Salem S. Salem; writing—review and editing: Mohammed Abu-Elghait, Mohamed K.Y. Soliman, Mohamed Salah Azab and Salem S. Salem; supervision: Mohammed Abu-Elghait, Mohamed Salah Azab and Salem S. Salem. All authors have read and agreed to the published version of the manuscript.

Funding Open access funding provided by The Science, Technology & Innovation Funding Authority (STDF) in cooperation with The Egyptian Knowledge Bank (EKB).

Data availability The data used to support the findings of this study are available from the corresponding author upon request.

Declarations

Ethics approval Not applicable.

Consent to participate Not applicable.

Consent for publication Not applicable.

Conflict of interest The authors declare no competing interests.

Open Access This article is licensed under a Creative Commons Attribution 4.0 International License, which permits use, sharing, adaptation, distribution and reproduction in any medium or format, as long as you give appropriate credit to the original author(s) and the source, provide a link to the Creative Commons licence, and indicate if changes were made. The images or other third party material in this article are included in the article’s Creative Commons licence, unless indicated otherwise in a credit line to the material. If material is not included in the article’s Creative Commons licence and your intended use is not permitted by statutory regulation or exceeds the permitted use, you will need to obtain permission directly from the copyright holder. To view a copy of this licence, visit <http://creativecommons.org/licenses/by/4.0/>.

References

- Ghosh S, Ahmad R, Zeyauallah M, Khare SK (2021) Microbial nano-factories: synthesis and biomedical applications. *Front Chem* 9. <https://doi.org/10.3389/fchem.2021.626834>
- Li X, Xu H, Chen Z-S, Chen G (2011) Biosynthesis of nanoparticles by microorganisms and their applications. *J Nanomater* 2011:270974. <https://doi.org/10.1155/2011/270974>
- Nayak S, Sajankila SP, Goveas LC, Rao VC, Mutalik S, Shreya BA (2020) Two fold increase in synthesis of gold nanoparticles assisted by proteins and phenolic compounds in *Pongamia* seed cake extract: response surface methodology approach. *SN Appl Sci* 2(4):634. <https://doi.org/10.1007/s42452-020-2348-5>
- Dezfuli AAZ, Abu-Elghait M, Salem SS (2023) Recent insights into nanotechnology in colorectal cancer. *Appl Biochem Biotechnol*. <https://doi.org/10.1007/s12010-023-04696-3>
- Soliman MKY, Salem SS, Abu-Elghait M, Azab MS (2023) Biosynthesis of silver and gold nanoparticles and their efficacy towards antibacterial, antibiofilm, cytotoxicity, and antioxidant activities. *Appl Biochem Biotechnol* 195(2):1158–1183. <https://doi.org/10.1007/s12010-022-04199-7>
- Huang X, El-Sayed MA (2010) Gold nanoparticles: optical properties and implementations in cancer diagnosis and photothermal therapy. *J Adv Res* 1(1):13–28. <https://doi.org/10.1016/j.jare.2010.02.002>
- Wen L, Lin Z, Gu P, Zhou J, Yao B, Chen G, Fu J (2009) Extracellular biosynthesis of monodispersed gold nanoparticles by a SAM capping route. *J Nanopart Res* 11:279–288
- Mařátková O, Michailidu J, Miřkovská A, Kolouchová I, Masák J, Čejková A (2022) Antimicrobial properties and applications of metal nanoparticles biosynthesized by green methods. *Biotechnol Adv* 58:107905. <https://doi.org/10.1016/j.biotechadv.2022.107905>
- Nayak S, Manjunatha K, Goveas LC, Rao CV, Sajankila SP (2021) Investigation of nonlinear optical properties of AgNPs synthesized using *Cyclea peltata* leaf extract post OVAT optimization. *BioNanoScience* 11(3):884–892
- Said A, Abu-Elghait M, Atta HM, Salem SS (2023) Antibacterial activity of green synthesized silver nanoparticles using *Lawsonia inermis* against common pathogens from urinary tract infection. *Appl Biochem Biotechnol*. <https://doi.org/10.1007/s12010-023-04482-1>
- Khan F, Shariq M, Asif M, Siddiqui MA, Malan P, Ahmad F (2022) Green nanotechnology: plant-mediated nanoparticle synthesis and application. *Nanomaterials* 12(4):673
- Nicolae-Maranciuc A, Chicea D, Chicea LM (2022) Ag nanoparticles for biomedical applications—synthesis and characterization—a review. *Int J Mol Sci* 23(10):5778
- Soliman MKY, Abu-Elghait M, Salem SS, Azab MS (2022) Multifunctional properties of silver and gold nanoparticles synthesis by *Fusarium pseudonygamai*. *Biomass Conv Bioref*. <https://doi.org/10.1007/s13399-022-03507-9>
- Al-Rajhi AMH, Salem SS, Alharbi AA, Abdelghany TM (2022) Ecofriendly synthesis of silver nanoparticles using Kei-apple (*Dovyalis caffra*) fruit and their efficacy against cancer cells and clinical pathogenic microorganisms. *Arab J Chem* 15(7):103927. <https://doi.org/10.1016/j.arabjc.2022.103927>
- Salem SS (2023) A mini review on green nanotechnology and its development in biological effects. *Arch Microbiol* 205(4):128. <https://doi.org/10.1007/s00203-023-03467-2>
- Rónavári A, Igaz N, Adamecz DI, Szerencsés B, Molnar C, Kónya Z, Pfeiffer I, Kiricsi M (2021) Green silver and gold nanoparticles: biological synthesis approaches and potentials for biomedical applications. *Molecules* 26(4):844
- Elakraa AA, Salem SS, El-Sayyad GS, Attia MS (2022) Cefotaxime incorporated bimetallic silver-selenium nanoparticles: promising antimicrobial synergism, antibiofilm activity, and bacterial

- membrane leakage reaction mechanism. *RSC Adv* 12(41):26603–26619. <https://doi.org/10.1039/D2RA04717A>
18. Xu F, Li Y, Zhao X, Liu G, Pang B, Liao N, Li H, Shi J (2023) Diversity of fungus-mediated synthesis of gold nanoparticles: properties, mechanisms, challenges, and solving methods. *Crit Rev Biotechnol*:1–17. <https://doi.org/10.1080/07388551.2023.2225131>
 19. Rana A, Yadav K, Jagadevan S (2020) A comprehensive review on green synthesis of nature-inspired metal nanoparticles: mechanism, application and toxicity. *J Clean Prod* 272:122880
 20. Salem SS, Hammad EN, Mohamed AA, El-DougDoug W (2023) A Comprehensive Review of Nanomaterials: Types, Synthesis, Characterization, and Applications. *Biointerface Res Appl Chem* 13(1). <https://doi.org/10.33263/BRIAC131.041>
 21. Salem SS, Ali OM, Reyad AM, Abd-ElSalam KA, Hashem AH (2022) *Pseudomonas indica*-Mediated Silver Nanoparticles: Antifungal and Antioxidant Biogenic Tool for Suppressing *Mucormycosis Fungi*. *J Fungi* 8(2):126. <https://doi.org/10.3390/jof8020126>
 22. Elfadel RG, Refat HM, El-Wahab HA, Salem SS, Owda ME, Abdel Reheim MAM (2023) Preparation of new surface coating based on modified oil-based polymers blended with ZnO and CuZnO NPs for steel protection. *Sci Rep* 13(1):7268. <https://doi.org/10.1038/s41598-023-34085-z>
 23. Salem SS (2022) Baker's yeast-mediated silver nanoparticles: characterisation and antimicrobial biogenic tool for suppressing pathogenic microbes. *BioNanoScience* 12(4):1220–1229. <https://doi.org/10.1007/s12668-022-01026-5>
 24. Lee KX, Shameli K, Yew YP, Teow SY, Jahangirian H, Rafiee-Moghaddam R, Webster TJ (2020) Recent developments in the facile bio-synthesis of gold nanoparticles (AuNPs) and their biomedical application. *Int J Nanomed* 15:275–300. <https://doi.org/10.2147/ijn.s233789>
 25. Salem SS (2022) Bio-fabrication of selenium nanoparticles using Baker's yeast extract and its antimicrobial efficacy on food borne pathogens. *Appl Biochem Biotechnol* 194(5):1898–1910. <https://doi.org/10.1007/s12010-022-03809-8>
 26. Abhishek S, Sneha N, Karthik P (2022) An emerging treatment technology: exploring deep learning and computer vision approach in revealing biosynthesized nanoparticle size for optimization studies. In: *Contaminants of Emerging Concerns and Reigning Removal Technologies*. CRC Press, pp 403–428
 27. Al-Zahrani FAM, Al-Zahrani NA, Al-Ghamdi SN, Lin L, Salem SS, El-Shishtawy RM (2022) Correction to: Synthesis of Ag/Fe₂O₃ nanocomposite from essential oil of ginger via green method and its bactericidal activity. *Biomass Conv Bioref*. <https://doi.org/10.1007/s13399-022-03353-9>
 28. Aref MS, Salem SS (2020) Bio-callsus synthesis of silver nanoparticles, characterization, and antibacterial activities via *Cinnamomum camphora* callus culture. *Biocatal Agric Biotechnol* 27:101689. <https://doi.org/10.1016/j.bcab.2020.101689>
 29. Al-Zahrani FAM, Salem SS, Al-Ghamdi HA, Nhari LM, Lin L, El-Shishtawy RM (2022) Green synthesis and antibacterial activity of Ag/Fe₂O₃ nanocomposite using *Buddleja lindleyana* extract. *Bioengineering* 9(9):452
 30. Abdelfattah NAH, Yousef MA, Badawy AA, Salem SS (n.d.) Influence of biosynthesized magnesium oxide nanoparticles on growth and physiological aspects of cowpea (*Vigna unguiculata* L.) plant, cowpea beetle, and cytotoxicity. *Biotechnol J n/a* (n/a):2300301. <https://doi.org/10.1002/biot.202300301>
 31. El-Khawaga AM, Elsayed MA, Gobara M, Soliman AA, Hashem AH, Zaher AA, Mohsen M, Salem SS (2023) Green synthesized ZnO nanoparticles by *Saccharomyces cerevisiae* and their antibacterial activity and photocatalytic degradation. *Biomass Conv Bioref*. <https://doi.org/10.1007/s13399-023-04827-0>
 32. Khalil AT, Ovais M, Iqbal J, Ali A, Ayaz M, Abbas M, Ahmad I, Devkota HP (2021) Microbes-mediated synthesis strategies of metal nanoparticles and their potential role in cancer therapeutics. *Semin Cancer Biol*. <https://doi.org/10.1016/j.semcancer.2021.06.006>
 33. Hashem AH, Khalil AMA, Reyad AM, Salem SS (2021) Biomedical applications of mycosynthesized selenium nanoparticles using *Penicillium expansum* ATTC 36200. *Biol Trace Elem Res* 199(10):3998–4008. <https://doi.org/10.1007/s12011-020-02506-z>
 34. Salem SS, Fouda A (2021) Green synthesis of metallic nanoparticles and their prospective biotechnological applications: an overview. *Biol Trace Elem Res* 199(1):344–370. <https://doi.org/10.1007/s12011-020-02138-3>
 35. Ponnurugan P (2017) Biosynthesis of silver and gold nanoparticles using *Trichoderma atroviride* for the biological control of Phomopsis canker disease in tea plants. *IET Nanobiotechnol* 11(3):261–267. <https://doi.org/10.1049/iet-nbt.2016.0029>
 36. Saha N, Trivedi P, Dutta Gupta S (2016) Surface plasmon resonance (SPR) based optimization of biosynthesis of silver nanoparticles from rhizome extract of *Curculigo orchioides* Gaertn. and its antioxidant potential. *J Cluster Sci* 27:1893–1912
 37. Rajivgandhi G, Gnanamangai BM, Prabha TH, Poornima S, Maruthupandy M, Alharbi NS, Kadaikunnan S, Li W-J (2022) Biosynthesized zinc oxide nanoparticles (ZnO NPs) using actinomycetes enhance the anti-bacterial efficacy against *K. Pneumoniae*. *J King Saud Univ-Sci* 34(1):101731
 38. Hammad EN, Salem SS, Mohamed AA, El-DougDoug W (2022) Environmental impacts of ecofriendly iron oxide nanoparticles on dyes removal and antibacterial activity. *Appl Biochem Biotechnol* 194:6053–6067. <https://doi.org/10.1007/s12010-022-04105-1>
 39. Ahmadi O, Jafarizadeh-Malmiri H, Jodeiri N (2018) Eco-friendly microwave-enhanced green synthesis of silver nanoparticles using *Aloe vera* leaf extract and their physico-chemical and antibacterial studies. *Green Process Synthesis* 7(3):231–240. <https://doi.org/10.1515/gps-2017-0039>
 40. Gutiérrez JM, González C, Maestro A, Solé I, Pey CM, Nolla J (2008) Nano-emulsions: new applications and optimization of their preparation. *Curr Opin Colloid Interface Sci* 13(4):245–251. <https://doi.org/10.1016/j.cocis.2008.01.005>
 41. Souril M, Hoseinpour V, Ghaemi N, Shakeri A (2019) Procedure optimization for green synthesis of manganese dioxide nanoparticles by *Yucca gloriosa* leaf extract. *Int Nano Lett* 9(1):73–81. <https://doi.org/10.1007/s40089-018-0257-z>
 42. Zhou J, Yu X, Ding C, Wang Z, Zhou Q, Pao H, Cai W (2011) Optimization of phenol degradation by *Candida tropicalis* Z-04 using Plackett-Burman design and response surface methodology. *J Environ Sci* 23(1):22–30
 43. Abdel-Fattah YR, Saeed HM, Gohar YM, El-Baz MA (2005) Improved production of *Pseudomonas aeruginosa* uricase by optimization of process parameters through statistical experimental designs. *Process Biochem* 40(5):1707–1714
 44. Jabeur F, Mechri S, Kriaa M, Gharbi I, Bejaoui N, Sadok S, Jaouadi B (2020) Statistical experimental design optimization of microbial proteases production under co-culture conditions for chitin recovery from speckled shrimp *Metapenaeus monoceros* by-product. *Biomed Res Int* 2020:3707804. <https://doi.org/10.1155/2020/3707804>
 45. Shin HS, Choi HC, Jung Y, Kim SB, Song HJ, Shin HJ (2004) Chemical and size effects of nanocomposites of silver and polyvinyl pyrrolidone determined by X-ray photoemission spectroscopy. *Chem Phys Lett* 383(3–4):418–422
 46. Xiong Y-H, Liu J-Z, Song H-Y, Ji L-N (2004) Enhanced production of extracellular ribonuclease from *Aspergillus niger* by optimization of culture conditions using response surface methodology. *Biochem Eng J* 21(1):27–32
 47. Barabadi H, Honary S, Ebrahimi P, Mohammadi MA, Alizadeh A, Naghibi F (2014) Microbial mediated preparation,

- characterization and optimization of gold nanoparticles. *Braz J Microbiol* 45:1493–1501
48. Könen-Adıgüzel S, Adıgüzel AO, Ay H, Alpdoğan S, Şahin N, Çaputçu A, Ergene RS, MetinGübür H, Tunçer M (2018) Genotoxic, cytotoxic, antimicrobial and antioxidant properties of gold nanoparticles synthesized by *Nocardia* sp. GTS18 using response surface methodology. *Mater Res Exp* 5(11):115402. <https://doi.org/10.1088/2053-1591/aadcc4>
 49. Brown AN, Smith K, Samuels TA, Lu J, Obare SO, Scott ME (2012) Nanoparticles functionalized with ampicillin destroy multiple-antibiotic-resistant isolates of *Pseudomonas aeruginosa* and *Enterobacter aerogenes* and methicillin-resistant *Staphylococcus aureus*. *Appl Environ Microbiol* 78(8):2768–2774. <https://doi.org/10.1128/AEM.06513-11>
 50. Dil EA, Ghaedi M, Ghaedi A, Asfaram A, Jamshidi M, Purkait MK (2016) Application of artificial neural network and response surface methodology for the removal of crystal violet by zinc oxide nanorods loaded on activate carbon: kinetics and equilibrium study. *J Taiwan Inst Chem Eng* 59:210–220
 51. Kittikunapong C, Ye S, Magadán-Corpas P, Pérez-Valero Á, Villar CJ, Lombó F, Kerkhoven EJ (2021) Reconstruction of a genome-scale metabolic model of *Streptomyces albus* j1074: Improved engineering strategies in natural product synthesis. *Metabolites* 11(5):304
 52. Kuhl M, Gläser L, Rebets Y, Rückert C, Sarkar N, Hartsch T, Kalinowski J, Luzhetskyy A, Wittmann C (2020) Microparticles globally reprogram *Streptomyces albus* toward accelerated morphogenesis, streamlined carbon core metabolism, and enhanced production of the antituberculosis polyketide pamamycin. *Biotechnol Bioeng* 117(12):3858–3875
 53. El-Ghwas DE, Mazeed TE, El-Waseif A, Al-Zahrani HA, Almaghrabi OA, Elazazy AM (2020) Factorial experimental design for optimization of zinc oxide nanoparticles production. *Curr Nanosci* 16(1):51–61
 54. Kaushik R, Saran S, Isar J, Saxena R (2006) Statistical optimization of medium components and growth conditions by response surface methodology to enhance lipase production by *Aspergillus carneus*. *J Mol Catal B Enzym* 40(3–4):121–126
 55. Othman AM, Elsayed MA, Elshafei AM, Hassan MM (2017) Application of response surface methodology to optimize the extracellular fungal mediated nanosilver green synthesis. *J Genet Eng Biotechnol* 15(2):497–504
 56. Bagewadi ZK, Mulla SI, Ninnekar HZ (2018) Optimization of endoglucanase production from *Trichoderma harzianum* strain HZN11 by central composite design under response surface methodology. *Biomass Conv Bioref* 8:305–316
 57. Hasnain MS, Javed MN, Alam MS, Rishishwar P, Rishishwar S, Ali S, Nayak AK, Beg S (2019) Purple heart plant leaves extract-mediated silver nanoparticle synthesis: optimization by Box-Behnken design. *Mater Sci Eng C* 99:1105–1114. <https://doi.org/10.1016/j.msec.2019.02.061>
 58. OndariNyakundi E, Padmanabhan MN (2015) Green chemistry focus on optimization of silver nanoparticles using response surface methodology (RSM) and mosquitocidal activity: *Anopheles stephensi* (Diptera: Culicidae). *Spectrochim Acta Part A Mol Biomol Spectrosc* 149:978–984. <https://doi.org/10.1016/j.saa.2015.04.057>
 59. Jiang H, Guo R, Mia R, Zhang H, Lü S, Yang F, Mahmud S, Liu H (2022) Eco-friendly dyeing and finishing of organic cotton fabric using natural dye (gardenia yellow) reduced-stabilized nanosilver: full factorial design. *Cellulose* 29(4):2663–2679. <https://doi.org/10.1007/s10570-021-04401-9>
 60. Obayori OS, Adebuseye SA, Ilori MO, Oyetibo GO, Omotayo AE, Amund OO (2010) Effects of corn steep liquor on growth rate and pyrene degradation by *Pseudomonas* strains. *Curr Microbiol* 60:407–411
 61. Ponnusami V, Krithika V, Madhuram R, Srivastava S (2007) Biosorption of reactive dye using acid-treated rice husk: factorial design analysis. *J Hazard Mater* 142(1–2):397–403
 62. Shakouri V, Salouti M, Mohammadi B, Zonooz NF (2016) Procedure optimization for increasing biosynthesis rate of gold nanoparticles by *Aspergillus flavus* supernatant. *Synth React Inorg, Met-Org, Nano-Met Chem* 46(10):1468–1472
 63. El Domany EB, Essam TM, Ahmed AE, Farghali AA (2018) Biosynthesis physico-chemical optimization of gold nanoparticles as anti-cancer and synergetic antimicrobial activity using *Pleurotus ostreatus* fungus. *J Appl Pharm Sci* 8(5):119–128
 64. Rane AN, Baikar VV, Ravi Kumar V, Deopurkar RL (2017) Agro-industrial wastes for production of biosurfactant by *Bacillus subtilis* ANR 88 and its application in synthesis of silver and gold nanoparticles. *Front Microbiol* 8:492
 65. Barabadi H, Honary S, Ebrahimi P, Alizadeh A, Naghibi F, Saravanan M (2019) Optimization of myco-synthesized silver nanoparticles by response surface methodology employing Box-Behnken design. *Inorgan Nano-Metal Chem* 49(2):33–43

Publisher's Note Springer Nature remains neutral with regard to jurisdictional claims in published maps and institutional affiliations.